

# Achieving a Superlong Lifetime in the Zeolite-Catalyzed MTO Reaction under High Pressure: Synergistic Effect of Hydrogen and Water

Xuebin Zhao,<sup>†,‡,§,⊥</sup> Jinzhe Li,<sup>†,⊥</sup> Peng Tian,<sup>\*,†</sup> Linying Wang,<sup>†</sup> Xiaofang Li,<sup>†,‡</sup> Shanfan Lin,<sup>†,‡</sup> Xinwen Guo,<sup>§</sup> and Zhongmin Liu<sup>\*,†</sup>

<sup>†</sup>National Engineering Laboratory for Methanol to Olefins, Dalian National Laboratory for Clean Energy, iChEM (Collaborative Innovation Center of Chemistry for Energy Materials), Dalian Institute of Chemical Physics, Chinese Academy of Sciences, Dalian 116023, P. R. China

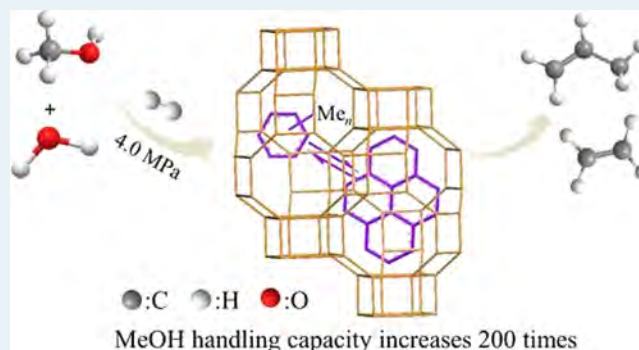
<sup>‡</sup>University of Chinese Academy of Sciences, Beijing 100049, P. R. China

<sup>§</sup>State Key Laboratory of Fine Chemicals, PSU-DUT Joint Center for Energy Research, School of Chemical Engineering, Dalian University of Technology, Dalian 116024, P. R. China

## Supporting Information

**ABSTRACT:** Zeolites are usually considered to be acid catalysts, which are prone to deactivation due to the coke deposition in the hydrocarbon conversions such as methanol-to-olefins (MTO) reaction. Herein, a high-pressure MTO process with cofeeding H<sub>2</sub> and H<sub>2</sub>O is reported, which can effectively prolong the catalytic lifetime of SAPO-34. The corresponding methanol handling capacity is about 200 times larger than that under the normal-pressure condition. Investigation reveals that the ultralong lifetime originates from the hydrogenation ability of the acid sites on SAPO-34 for aromatic species, which can hydrogenate the heavy aromatic deposits (especially the phenanthrene composed of three benene rings) to active aromatic intermediates (methylbenzenes and methylnaphthalenes) and thus slow down the evolution of coke species. A positive synergistic effect between H<sub>2</sub> and H<sub>2</sub>O on prolonging the catalyst lifetime is observed at higher H<sub>2</sub>O partial pressure, likely resulting from the reduced barriers of hydrogenation reactions in the presence of H<sub>2</sub>O. Furthermore, the evolution pathways of coke species are markedly affected by reaction temperature, and fast deactivation may occur below 400 °C due to the formation of large molecule diadamantanes.

**KEYWORDS:** methanol to olefins, SAPO-34, long lifetime, high-pressure H<sub>2</sub>, hydrogenation



## 1. INTRODUCTION

Zeolites are important crystalline materials with uniform pores and tunable acidity, which have been widely used as acid catalysts in the chemical industry. A common feature associated with the zeolite catalysts is the deactivation phenomenon because the acid sites on zeolites not only are active for the target reaction but also tend to cause a coke deposition.<sup>1</sup> The general approach of solving this problem is to adopt fluidized bed reactor to realize the frequent regeneration of the catalyst. In addition, preparation of metal–zeolite composite catalysts is proposed to improve the intrinsic lifetime of the catalysts, which combines the acid properties of zeolite and the hydrogenation ability of metal component. Notable applications include the hydrocracking catalysts and C<sub>8</sub> aromatics isomerization catalysts. However, the hydrogenation ability of zeolite has drawn less attention and recognition until now. It has been proven that alkenes such

as ethene can be hydrogenated on the Brønsted acid sites by experimental<sup>2,3</sup> and theoretical<sup>4,5</sup> studies. Arenes, such as benzene (or protonated benzene), hardly react with hydrogen unless there exists a tertiary hydride source, which can transfer a hydride to protonated benzene.<sup>6</sup>

The methanol-to-olefins (MTO) transformation catalyzed by zeolites is one of the most important processes in C1 chemistry, which provides an alternative route to produce light olefins from nonoil resources such as coal and nature gas. Commercial DMTO process with a production capacity of a million tons of light olefins per year has been successfully put into operation based on the SAPO-34 catalyst since 2010.<sup>7</sup> Intensive studies have demonstrated that light olefins are

Received: November 1, 2018

Revised: February 23, 2019

Published: February 25, 2019

generated through a hydrocarbon pool (HCP) mechanism.<sup>8,9</sup> Specifically, methylbenzenes and the corresponding carbenium ions confined in SAPO-34 cavities are the main reactive intermediates (HCP species), to which methanol is continuously added and from which light olefins are eliminated.<sup>10–12</sup> However, the HCP species generated on the acid sites in cages of SAPO-34 tend to grow larger into polycyclic aromatics, which could not diffuse to gas phase due to the narrow eight-ring pore openings of SAPO-34.<sup>13</sup> Such evolution of aromatic species is generally completed within a few hours over SAPO-34 and leads to the deactivation, so that the commercial MTO process has to adopt the circulating fluidized bed system. One fundamental and important question is whether the evolution of aromatic species confined in the cavities of SAPO-34 can be controlled to achieve long or even undying lifetime.

The idea of exploring the SAPO-34-catalyzed MTO reaction under high pressure of H<sub>2</sub> and water was inspired by the recent reports of selective conversion of syngas to light olefins (STO)<sup>14,15</sup> over oxide-SAPO-34 bifunctional catalyst. Compared with the MTO reaction, the STO reaction shows a much longer lifetime of at least 100 h, and the products distribution moves backward with propene as the major product (about 45%). The CO activation and C–C bond coupling are proposed to occur on metal oxide and zeolite, respectively, although the intermediate species (ketene<sup>14,16</sup> or methanol<sup>15,17–19</sup>) responsible for the light olefins formation over SAPO-34 are still in controversy. Because acetyl group (a physisorbed protonated ketene on Brønsted acid sites) has been demonstrated to exist in the MTO reaction and links the direct and HCP mechanisms,<sup>20</sup> it seems that the reaction precursor over SAPO-34 in the STO process is comparable to that in the MTO process. The difference is that the STO reaction is carried out under the atmosphere of H<sub>2</sub> and CO. This suggests the possibility of prolonging the MTO lifetime of SAPO-34 by cofeeding additional gases.

In the present work, we report that the lifetime in the MTO reaction over zeolite can be greatly prolonged by cofeeding high-pressure H<sub>2</sub> and H<sub>2</sub>O mixture (named as H-DMTO process). During our manuscript preparation, Bhan et al. reported a lifetime improvement in the MTO reaction on SAPO-34 by only H<sub>2</sub> cofeeds;<sup>21</sup> however, here a synergistic effect between H<sub>2</sub> and H<sub>2</sub>O on prolonging the catalyst lifetime is observed, and the intrinsic reason for the lifetime extension is investigated. The acid sites of SAPO-34 are revealed to have strong catalytic hydrogenation ability for olefins and aromatic deposits confined in the cavities, which slows down the growth rate of polycyclic aromatics and increases the catalytic stable period of SAPO-34. Furthermore, the influence of reaction temperature and contact time on the H-DMTO reaction has been investigated.

## 2. EXPERIMENTAL SECTION

**2.1. Catalyst and Characterizations.** SAPO-34 was provided by DNL1202 Group in Dalian Institute of Chemical Physics, Chinese Academy of Sciences. The powder XRD pattern was recorded on a PANalytical X'Pert PRO X-ray diffractometer with Cu–K $\alpha$  radiation ( $\lambda = 0.15418$  nm), operating at 40 kV and 40 mA. The chemical composition of solid samples was determined with a PhilipsMagix-601 X-ray fluorescence (XRF) spectrometer. The crystal morphology was observed using a scanning electron microscope (Hitachi SU8020). N<sub>2</sub> adsorption–desorption isotherms at  $-196$  °C were determined on a Micromeritics ASAP2020. Prior to the

measurement, samples were degassed at 350 °C under vacuum for 4 h. The total surface area was calculated based on the BET equation. Temperature-programmed desorption of ammonia (NH<sub>3</sub>-TPD) was measured on a Micrometric 2920 chemical adsorption instrument. Each sample (40–60 mesh, 0.20 g) was loaded into a quartz U-shaped reactor and pretreated at 600 °C for 1 h in flowing He. After the pretreatment, the sample was cooled to 100 °C and saturated with NH<sub>3</sub> gas. Then, NH<sub>3</sub>-TPD was carried out in a constant flow of He (20 mL min<sup>-1</sup>) from 100 to 550 °C at a heating rate of 10 °C min<sup>-1</sup>.

All solid-state NMR experiments were performed using a Bruker Avance III 600 spectrometer equipped with a 14.1 T wide-bore magnet. The resonance frequencies in this field strength were 156.4, 242.9, and 119.2 MHz for <sup>27</sup>Al, <sup>31</sup>P, and <sup>29</sup>Si, respectively. The <sup>29</sup>Si MAS NMR spectra were recorded at a spinning rate of 8 kHz using high-power proton decoupling. One thousand twenty-four scans were accumulated, with a  $\pi/4$  pulse width of 2.5  $\mu$ s and a 10 s recycle delay. Chemical shifts were referenced to 4,4-dimethyl-4-silapentanesulfonate sodium salt (DSS). <sup>27</sup>Al MAS NMR spectra were recorded at a spinning rate of 12 kHz using one pulse sequence. Two hundred scans were accumulated, with a  $\pi/8$  pulse width of 0.75  $\mu$ s and a 2 s recycle delay. Chemical shifts were referenced to (NH<sub>4</sub>)Al(SO<sub>4</sub>)<sub>2</sub>·12 H<sub>2</sub>O at  $-0.4$  ppm. The <sup>31</sup>P MAS NMR spectra were recorded using high-power proton decoupling. Thirty-two scans were accumulated with a  $\pi/4$  pulse width of 2.25  $\mu$ s and a 10 s recycle delay. Chemical shifts were referenced to 85% H<sub>3</sub>PO<sub>4</sub> at 0 ppm.

**2.2. Catalytic Reaction Test.** The as-made SAPO-34 was pressed and sieved to 40–60 mesh, and the organic template in the product was removed by calcination at 650 °C for 2 h. Calcined catalyst (0.5 g) was loaded in a fixed-bed stainless steel reactor with inner diameter of 10 mm. After boosting to the reaction pressure, the catalyst was activated at 500 °C for 60 min under carrier gas, and then the temperature was adjusted to reaction temperature. Methanol aqueous solution was fed by a pump, which gave a methanol WHSV of 4.0 h<sup>-1</sup>. The effluent products from reactor were kept warm and analyzed by an online Agilent 7890A GC equipped with a Pora PLOT-Q-HT capillary column (27.5 m  $\times$  0.32 mm  $\times$  10  $\mu$ m) and a Porapak QS packed column (3 m  $\times$  2 mm). The conversion and selectivity were calculated on CH<sub>2</sub> basis. Dimethyl ether (DME) was considered as reactant in the calculation. The reaction lifetime is defined as the duration of >99% methanol conversion.

**2.3. Confined Organics Determination with GC-MS.** The discharged catalysts were analyzed by thermogravimetric analysis (TGA), and the loss between 300 and 700 °C was used to estimate the coke content. For the coke species, 50.0 mg of discharged catalyst was dissolved in 1.0 mL of 40% HF solution and extracted with 1.0 mL of CH<sub>2</sub>Cl<sub>2</sub> with C<sub>2</sub>Cl<sub>6</sub> (200 ppm) as interior label. After neutralization and separation, the CH<sub>2</sub>Cl<sub>2</sub> solution was identified by a GC-MS equipped with a HP-5 capillary column and an FID detector. Moreover, the compounds with molecular weight greater than 200 in the CH<sub>2</sub>Cl<sub>2</sub> solution were also detected by a 15-T SolariX XR FTICR mass spectrometer (Bruker Daltonics, Bremen, Germany) using 1,8,9-anthracenetriol (dithranol) as a matrix. The instrument was equipped with a Nd:YAG laser ( $\lambda = 355$  nm) and a time-of-flight mass analyzer in reflection mode. Positive ion mass spectra were recorded in the mass region between 200 and 1500 Da.

### 3. RESULTS AND DISCUSSION

**3.1. Synergistic Effect between H<sub>2</sub> and H<sub>2</sub>O under High Pressure.** The physicochemical properties of SAPO-34 used for the high-pressure MTO reaction are shown in Figure S1 and Table S1, which evidence the good crystallinity and single Si(4Al) environment of the material with an acid density of 0.81 mmol/g.

Figure 1 presents the effects of different atmospheres (N<sub>2</sub>, H<sub>2</sub>, H<sub>2</sub>O, and H<sub>2</sub>–H<sub>2</sub>O mixture) on the reaction over SAPO-

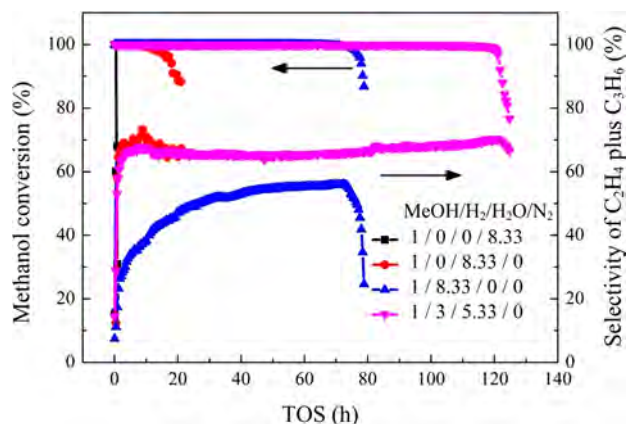


**Figure 1.** Synergistic effect between H<sub>2</sub>O and H<sub>2</sub> on the catalytic performance of SAPO-34 in the H-DMTO process. Reaction conditions: 450 °C, 4.0 MPa, methanol WHSV = 4.0 h<sup>-1</sup>, GHSV = 13 069 h<sup>-1</sup>, contact time = 4.2 s.

34 catalyst. Under N<sub>2</sub> atmosphere ( $P_{N_2} = 3.57$  MPa), SAPO-34 deactivates very fast. Under pure H<sub>2</sub>O atmosphere ( $P_{H_2O} = 3.57$  MPa), the lifetime of SAPO-34 is extended to 15 h, which can be attributed to the inhibition of hydrogen transfer reactions by the competitive adsorption of H<sub>2</sub>O over acid sites.<sup>22–24</sup> Under H<sub>2</sub> condition ( $P_{H_2} = 3.57$  MPa), the catalyst lifetime is further prolonged (75 h) which possibly originates from the catalytic hydrogenation ability of SAPO-34 but with an obvious decrease of C<sub>2</sub>H<sub>4</sub> plus C<sub>3</sub>H<sub>6</sub> selectivity due to the formation of C<sub>2</sub>H<sub>6</sub> and C<sub>3</sub>H<sub>8</sub>. Interestingly, under H<sub>2</sub> and H<sub>2</sub>O coexisting condition ( $P_{H_2} + P_{H_2O} = 3.57$  MPa), the lifetime of SAPO-34 can reach 118 h, which is much longer than that under pure H<sub>2</sub> or pure H<sub>2</sub>O atmosphere; the selectivity of C<sub>2</sub>H<sub>4</sub> plus C<sub>3</sub>H<sub>6</sub> is also higher than that of pure H<sub>2</sub> atmosphere. This demonstrates that the coexistence of H<sub>2</sub>O and H<sub>2</sub> can generate a positive synergistic effect on the MTO reaction over SAPO-34, which will be further studied in the following sections.

Figure S2 shows the coke analysis of the deactivated SAPO-34 under different atmospheres. The coke species detected by GC-MS herein are similar to those of the normal-pressure reaction at 450 °C,<sup>13,25,26</sup> which mainly consist of polycyclic aromatics (phenanthrenes and pyrenes). Little difference can be found among the four catalysts. However, the coke amount and coke deposition rate on the catalysts show obvious difference (Table S2), depending on the reaction atmospheres. The catalyst under pure N<sub>2</sub> atmosphere has an extremely fast coke deposition rate, which is consistent with its short catalytic lifetime. With the presence of H<sub>2</sub> or H<sub>2</sub>O in the reaction system, the coke deposition rate decreases obviously. However, the total coke amount on the catalyst under pure H<sub>2</sub> atmosphere is unexpectedly high (74.2%). Large amount of

coke exists on the exterior of the catalyst, indicating that high-pressure H<sub>2</sub> cannot suppress the coke growth on the external surface of the catalyst. Further investigation is needed to find out the intrinsic reason for this. The H<sub>2</sub>–H<sub>2</sub>O cofeeding system gives the lowest coke deposition rate of 2.0 mg/(g·h) with a coke amount of 19.7%. The greatly reduced coke deposition rate under H<sub>2</sub>–H<sub>2</sub>O condition agrees with its long lifetime and confirms the existence of synergistic effect between H<sub>2</sub>O and H<sub>2</sub>.

**3.2. The Effect of H<sub>2</sub> Partial Pressure and H<sub>2</sub>O Partial Pressure.** The effect of H<sub>2</sub> in the H<sub>2</sub>–H<sub>2</sub>O cofeeding condition on the catalytic performance of SAPO-34 is studied by altering the H<sub>2</sub> partial pressure ( $P_{H_2}$ ). N<sub>2</sub> is used as equilibrium gas to maintain the same contact time (CT). As shown in Figures 2a and S3, the reaction lifetime shows an

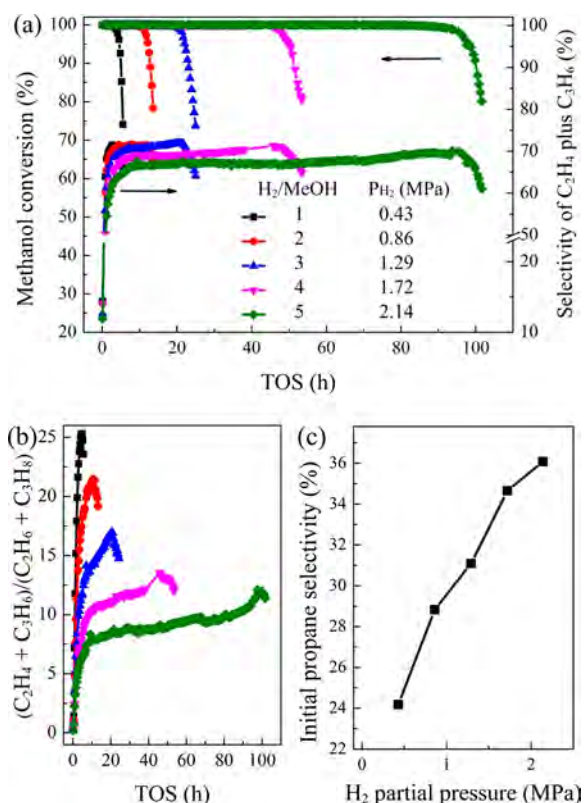


**Figure 2.** Effect of H<sub>2</sub> partial pressure on (a) methanol conversion and olefins selectivity, (b) (C<sub>2</sub>H<sub>4</sub> + C<sub>3</sub>H<sub>6</sub>)/(C<sub>2</sub>H<sub>6</sub> + C<sub>3</sub>H<sub>8</sub>) ratio (O/P ratio), and (c) initial propane selectivity (TOS = 0.43 h) over SAPO-34. Reaction conditions: 450 °C, 4.0 MPa, H<sub>2</sub>/MEOH/H<sub>2</sub>O/N<sub>2</sub> =  $x/1/2.67/y$ ,  $x + y = 5.66$ , methanol WHSV = 4.0 h<sup>-1</sup>, GHSV = 13 069 h<sup>-1</sup>, contact time = 4.2 s.

obvious extension from 3 to 93 h when the  $P_{H_2}$  increases from 0.43 to 2.14 MPa; the selectivity of C<sub>2</sub>H<sub>4</sub> plus C<sub>3</sub>H<sub>6</sub> drops gradually with the rising of  $P_{H_2}$ , together with a corresponding increase of alkanes selectivity (C<sub>2</sub>H<sub>6</sub> and C<sub>3</sub>H<sub>8</sub>). For the normal-pressure MTO reaction, high alkane selectivity is always accompanied by short reaction lifetime due to hydrogen transfer reactions. However, herein both reaction lifetime and alkanes selectivity give an increasing trend with the rising  $P_{H_2}$ , suggesting that the alkanes, at least part of them, should not be from the hydrogen transfer reactions. On the other hand, C<sub>3</sub>H<sub>6</sub> is the dominant product, followed by C<sub>2</sub>H<sub>4</sub> and C<sub>4</sub>. The



products distribution is different from the normal-pressure MTO reaction ( $C_2H_4$  and  $C_3H_6$  as the major products) but similar to that of the high-pressure reaction under the  $H_2$ -absent atmosphere (Figure S4). It is speculated that the increased contact time and methanol partial pressure<sup>27–30</sup> under high pressure may play important roles in determining the product carbon distribution. On the whole, the selectivities of ( $C_2H_4 + C_3H_6$ ) (66–72%) and ( $C_2H_4 + C_3H_6 + C_4$ ) (82–86%) at the stable period in the H-DMTO process are less than those of the normal-pressure MTO reaction (Figure S4) but much closer to those of the reported high-pressure STO process.<sup>14,15</sup>

The corresponding olefins/paraffins (O/P) ratios are calculated and illustrated in Figure 2b, and the initial propane selectivity is shown in Figure 2c. It can be seen that the O/P ratios decrease with the rising  $P_{H_2}$ , while initial propane selectivity increases obviously, which suggests the occurrence of the direct hydrogenation of olefin products over SAPO-34,<sup>2,4,5</sup> and the hydrogenation degree is proportional to the  $P_{H_2}$ . Moreover, the O/P ratios display a greatly increasing trend with the TOS. It is speculated that the fresh SAPO-34 catalyst may have the strongest ability for olefins hydrogenation, and the hydrogenation activity drops as the reaction proceeds likely due to the coverage of the strong acid sites by coke. Table S3 lists the coke deposition rates under different  $P_{H_2}$ . A dropping trend can be observed from 58.9 to 8.9 mg/(g·h) with the increase of  $P_{H_2}$  from 0.43 to 2.14 MPa, which implies the increasing inhibition on the coke deposition and agrees with the corresponding reaction lifetime.

The reactions under pure  $H_2$  atmosphere with different  $P_{H_2}$  have also been investigated and are presented in Figure S5. It can be seen that the catalytic lifetime increases sharply with the increase of the  $P_{H_2}$  while the selectivity of  $C_2H_4$  plus  $C_3H_6$  gives a dropping trend. These are similar to the results of increasing  $P_{H_2}$  in  $H_2$ – $H_2O$  cofeeding system (Figure 2) and indicate the enhanced catalytic hydrogenation ability of SAPO-34. However, when comparing the results in Figure S5 and Figure 2 with the same  $H_2$  partial pressure (e.g.,  $P_{H_2} = 1.29$  MPa), both the olefins selectivity and reaction lifetime under pure  $H_2$  atmosphere are inferior to those of the  $H_2$ – $H_2O$  system, showing the positive effect of water on the reaction.

The effect of  $H_2O$  partial pressure ( $P_{H_2O}$ ) on the H-DMTO reaction is shown in Figure 3. Under the investigated conditions, the catalytic lifetime is prolonged from 3.4 to 20.6 h when increasing the  $P_{H_2O}$  from 0 to 1.15 MPa; it is further prolonged significantly to 118 h when  $P_{H_2O}$  increases to 2.29 MPa. The selectivity of  $C_2H_4$  plus  $C_3H_6$  presents a rising trend from  $P_{H_2O} = 0$  to 1.15 MPa but decreases when further increasing the  $P_{H_2O}$  to 2.29 MPa. The corresponding O/P ratios and initial propane selectivity also show a turning point at  $P_{H_2O} = 1.15$  MPa, implying that the hydrogenation ability of SAPO-34 for olefin products drops first and then rises following the increase of  $P_{H_2O}$  despite the unchanged  $H_2$  partial pressure. The corresponding coke content and coke deposition rate of the deactivated catalysts are listed in Table S4. The coke deposition rate decreases from 36.3 to 2.0 mg/(g·h) with the rising of  $P_{H_2O}$  from 0 to 2.29 MPa, indicating an enhanced inhibition on the coke deposition.

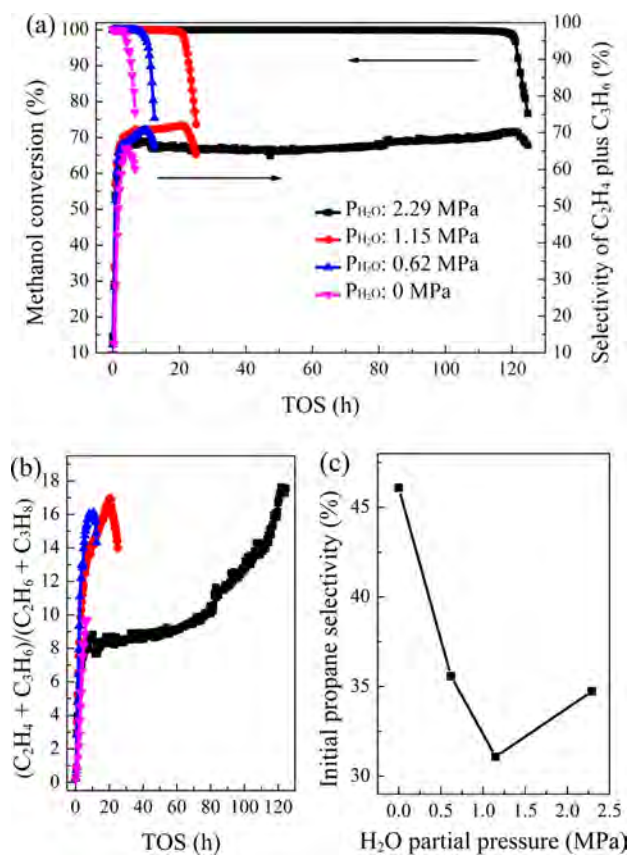


**Figure 3.** Effect of  $H_2O$  partial pressure on (a) methanol conversion and olefins selectivity, (b)  $(C_2H_4 + C_3H_6)/(C_2H_6 + C_3H_8)$  ratio (O/P ratio), and (c) initial propane selectivity (TOS = 0.43 h) over SAPO-34. Reaction conditions: 450 °C, 4.0 MPa,  $H_2/MEOH/H_2O/N_2 = 3/1/x/y$ ,  $x + y = 5.66$ , methanol WHSV = 4.0  $h^{-1}$ , GHSV = 13 069  $h^{-1}$ , contact time = 4.2 s.

To better understand the effect of  $H_2O$  in the system, the catalytic performance of SAPO-34 under pure  $H_2O$  atmosphere is investigated and shown in Figure S5. A positive effect on the lifetime improvement is found following the increase of  $P_{H_2O}$ , and the selectivity of  $C_2H_4$  plus  $C_3H_6$  remains almost unchanged. Similar phenomena have been reported before for the normal-pressure MTO reaction, in which an increase of light olefins selectivity and moderate prolonging of lifetime were observed. It was ascribed to the strong competitive adsorption of water on the Brønsted acid sites, which reduces the growth rate of coke species.<sup>24,31,32</sup> This is consistent with the observation in the H-DMTO reaction at relatively low  $P_{H_2O}$  (0–1.15 MPa) but fails to explain the decreased light olefins selectivity when further increasing the  $P_{H_2O}$  to 2.29 MPa (Figure 3). According to the literature, water can protonate the acid sites to form hydronium ( $H_3O^+$ ) ions,<sup>33</sup> and  $H_3O^+$  can dramatically diminish the barrier of hydrogenation reaction,<sup>5</sup> which seems a plausible explanation for the positive synergetic effect of  $H_2O$  and  $H_2$  in the H-DMTO process.

**3.3. The Catalytic Hydrogenation of Aromatics on SAPO-34.** So far, there is no evidence for the aromatics hydrogenation on acidic zeolites, although olefins hydrogenation on acidic zeolites has been demonstrated.<sup>2,4,5</sup> This is due to the higher difficulty of aromatics hydrogenation than olefins hydrogenation.<sup>34</sup> Previous literature once reported that aromatics hydrogenation could take place over strong acid

such as  $\text{HCl-AlCl}_3$ <sup>6,35</sup> and metal-free hydrogenation catalyst  $\text{B}(\text{C}_6\text{F}_5)_3/\text{Ph}_2\text{PC}_6\text{F}_5$  via a mechanism involving protonation of aromatic species followed by hydride transfer.<sup>36</sup> Given that aromatics confined in the cavities of SAPO-34 can generate corresponding carbenium ions readily, it is speculated that the aromatic carbenium ions may be hydrogenated under high-pressure  $\text{H}_2$  atmosphere on SAPO-34, which inhibits the coke deposition and thus significantly prolongs the reaction lifetime.

To confirm our speculation about the aromatics hydrogenation over SAPO-34, the deactivated catalyst is treated by high-pressure  $\text{H}_2$  at 450 °C. TG analysis indicates that more than 40% coke was eliminated after  $\text{H}_2$  treatment, producing  $\text{CH}_4$ ,  $\text{C}_2\text{H}_6$ , and  $\text{C}_3\text{H}_8$  as gas products (Figure S6 and Table S5). The coke species retained in the catalysts detected by GC-MS before and after the  $\text{H}_2$  treatment are shown in Figure 4.

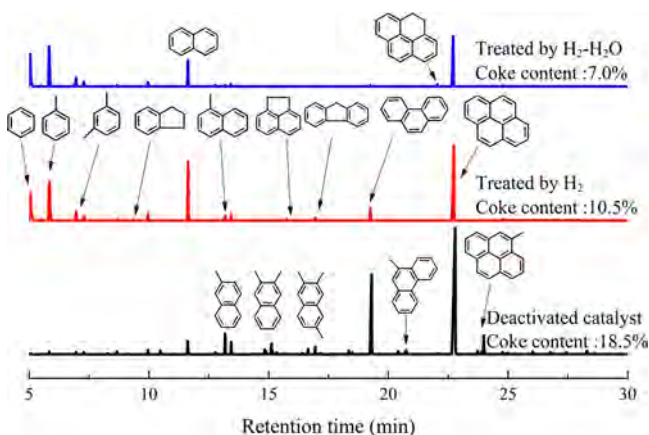


**Figure 4.** GC-MS chromatograms of organic species retained in the deactivated SAPO-34 catalysts before and after the  $\text{H}_2/\text{H}_2\text{O}$  treatments. Reaction conditions for the deactivated SAPO-34: 450 °C, 0.5 MPa,  $\text{N}_2/\text{MEOH}/\text{H}_2\text{O} = 1/1/2.67$ ,  $\text{GHSV} = 6541 \text{ h}^{-1}$ ;  $\text{H}_2$  treatment conditions: 450 °C, 4.0 MPa,  $\text{He}/\text{H}_2 = 6.33/3$ ,  $\text{GHSV} = 13\,069 \text{ h}^{-1}$ ;  $\text{H}_2\text{O}$  cofeeding treatment conditions: 450 °C, 4.0 MPa,  $\text{He}/\text{H}_2/\text{H}_2\text{O} = 1/3/5.33$ ,  $\text{GHSV} = 13\,069 \text{ h}^{-1}$ .

Upon the  $\text{H}_2$  treatment, the content of tri- and tetracyclic aromatics (especially the former species) drops with the increase of light aromatics. A small amount of light aromatics even possesses saturated rings (five- or six-membered rings). These phenomena are consistent with the change of coke species with molecular weight higher than 200 detected by FT-ICR-MS (Figure S7), showing that heavy aromatics are more active for the hydrogenation reaction than light aromatics, and the hydrogenation of polycyclic aromatics on SAPO-34 is accompanied by cracking reactions. The distinct hydrogenation reactivity of aromatic species is likely due to their different stability and steric structures.<sup>34</sup> The most interesting one is phenanthrene (the second abundant coke species in the deactivated SAPO-34 from GC-MS analysis), whose amount shows a dramatical decrease after the  $\text{H}_2$  treatment (Figure 4). Very recent theoretical investigation also confirms the phenanthrene hydrogenation over acidic MOR zeolite.<sup>37</sup>

To learn the possibility of aromatics hydrogenation on SAPO-34 with  $\text{H}_2\text{O}$  as the reductant, the deactivated catalyst was treated under high-pressure  $\text{H}_2\text{O}$  atmosphere at 450 °C (Figure S8). However, the total coke amount just shows a slight decrease after the treatment, and the coke species detected by GC-MS remain almost unchanged (Figure S8c), implying the weak effect of water on eliminating the coke.

Alkene ( $\text{C}_2\text{H}_4$ ) and CO are the main gas products with a small amount of  $\text{CH}_4$  and  $\text{C}_2\text{H}_6$  (Figure S8b), which further confirms that water has weak ability to act as a hydrogen source for hydrogenation reaction.

Furthermore,  $\text{H}_2\text{O}$ – $\text{H}_2$  mixture was also explored for the regeneration of the deactivated catalyst, and the results are given in Figure 4. Both the residual coke amount and the content of polycyclic aromatic species in the detectable coke species are lower than those of the  $\text{H}_2$ -treated catalyst, showing an enhanced catalytic hydrogenation ability under  $\text{H}_2\text{O}$ – $\text{H}_2$  cofeeding conditions. This confirms the positive synergetic effect between  $\text{H}_2\text{O}$  and  $\text{H}_2$ .

**3.4. The Effect of Reaction Temperature on the H-DMTO Reaction.** The effect of reaction temperature on the methanol conversion in the H-DMTO process is displayed in Figure 5a, and detailed product distributions are shown in

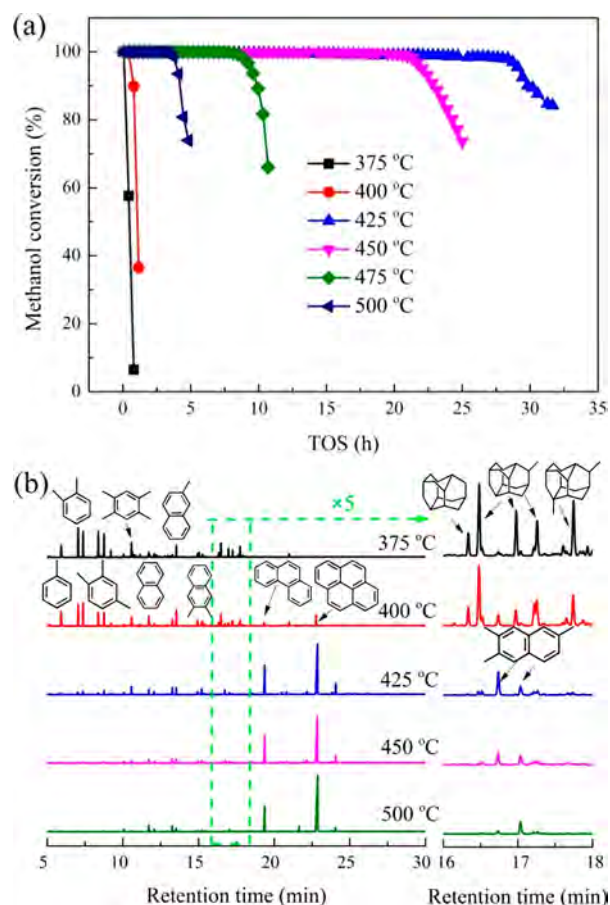


**Figure 5.** (a) Methanol conversion as a function of TOS at different reaction temperatures. Reaction conditions: 4.0 MPa,  $\text{H}_2/\text{MEOH}/\text{H}_2\text{O}/\text{N}_2 = 3/1/2.67/2.66$ , methanol  $\text{WHSV} = 4.0 \text{ h}^{-1}$ ,  $\text{GHSV} = 13\,069 \text{ h}^{-1}$ . (b) GC-MS chromatograms of the organic species retained in the deactivated catalysts.

Figure S9. Interestingly, the reaction at 375 and 400 °C displays an extremely short lifetime of less than 1 h; it reaches the maximum of 22.1 h at 425 °C and then decreases with the increase of reaction temperature. Considering the relatively little difference in the lifetime of the normal-pressure MTO reaction between 375 and 450 °C over SAPO-34,<sup>38</sup> it is supposed that the rapid deactivation at 375 and 400 °C herein should be closely related to the presence of  $\text{H}_2$ . The coke species and coke content on the deactivated catalysts are



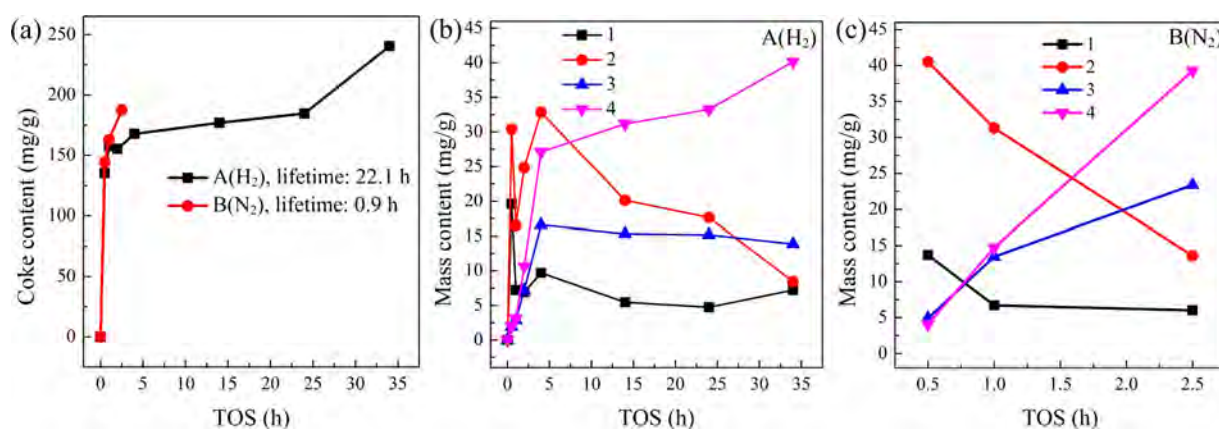
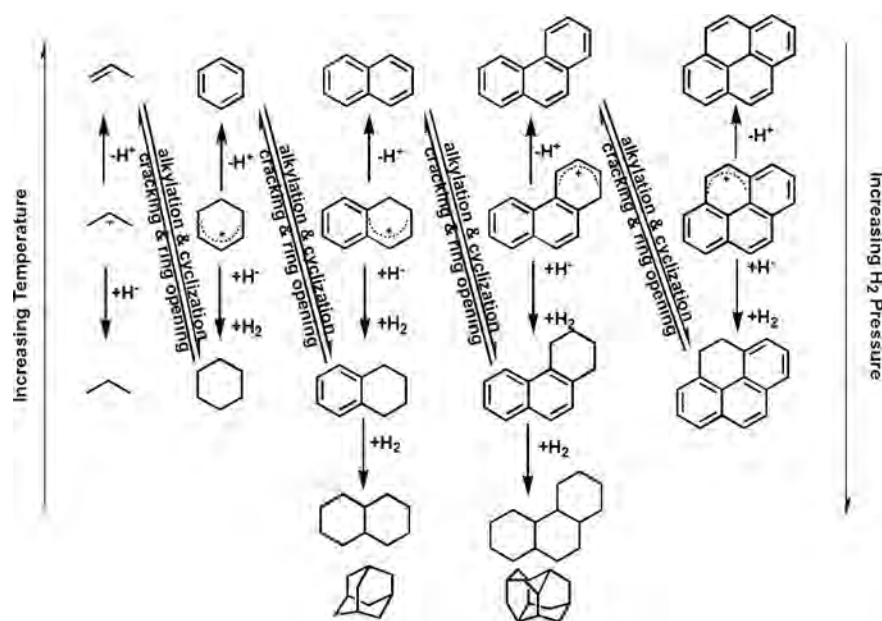


**Figure 6.** (a) Effect of reaction atmosphere on the evolution of coke content on SAPO-34 at 425 °C. The coke content is estimated by the weight loss between 300 and 700 °C at the TG curves. (b) Mass content of coke species with different benzene rings as a function of TOS under H<sub>2</sub> atmosphere. (c) Mass content of coke species with different benzene rings as a function of TOS under H<sub>2</sub>-absent atmosphere. 1: benzene and its methyl substitutes; 2: naphthalene and its methyl substitutes; 3: phenanthrene and its methyl substitutes; 4: pyrene and its methyl substitutes. Reaction conditions for A(H<sub>2</sub>): 425 °C, 4.0 MPa, H<sub>2</sub>/MEOH/H<sub>2</sub>O/N<sub>2</sub> = 3/1/2.67/2.66, methanol WHSV = 4.0 h<sup>-1</sup>, GHSV = 13 069 h<sup>-1</sup>. Reaction conditions for B(N<sub>2</sub>) are the same as those of A(H<sub>2</sub>) except the flow gas without H<sub>2</sub>, MEOH/H<sub>2</sub>O/N<sub>2</sub> = 1/2.67/5.66.

### Scheme 1. Proposed Evolution Network of Coke Species for Methanol Conversion over SAPO-34 Catalyst in H-DMTO Process



shown in Figure 5b and Table S6. Obviously, the coke deposition rates at lower temperatures are the highest, and the corresponding coke species are distinct from those at higher temperatures. The coke species at 375 and 400 °C are mainly centering on methylbenzenes and diadamantanes, while heavy cyclic aromatics become the dominant coke species at higher temperatures. It is unexpected to see the deactivated catalysts enriched with methylbenzenes (active intermediates for the MTO reaction). Likely, the formation of diadamantanes at 375 and 400 °C, which was not found before as the coke species for the MTO reaction, blocks the channels, increases the difficulty in mass transfer and thus causes the fast deactivation.

We further investigated the reaction performance at 400 °C under different H<sub>2</sub> partial pressures (Figure S10). Less change in catalytic lifetime can be discerned, confirming that the H-DMTO reaction at 400 °C is different from those at higher temperatures. An enhanced trend of diadamantanes, benzene,

and their methylsubstitutes in the coke species can be observed with the increase of P<sub>H<sub>2</sub></sub>, at the expense of the formation of phenanthrene and pyrene (Figure S10d). This evidences the strong inhibition of high P<sub>H<sub>2</sub></sub> on the growth of aromatic species. Moreover, the content of aromatic species with saturated rings such as hydrindene, tetralin, and diphenyl also shows an increasing trend with the rising of P<sub>H<sub>2</sub></sub> (Figure S10c), confirming that the aromatic species is hydrogenated over SAPO-34 in the H-DMTO process.

When the reaction temperature increases to 425 °C, long catalytic lifetime is observed (Figure 5a). The evolution of coke content with TOS is displayed in Figure 6. As a comparison, the results from the H<sub>2</sub>-absent atmosphere are also given in Figure 6a. Under the H-DMTO conditions, the coke content rises rapidly in the initial few hours, and then its increase becomes slow lasting for about 34 h. The final coke

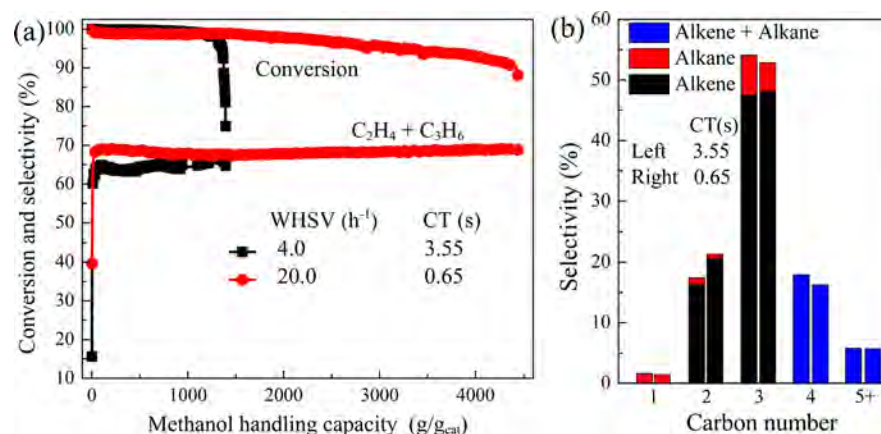


**Figure 7.** (a) Methanol conversion and products selectivity as a function of MHC on SAPO-34. (b) Products distribution at MHC = 200 g/g<sub>cat</sub>. Reaction conditions for CT = 0.65 s: 425 °C, 4.0 MPa, H<sub>2</sub>/MEOH/H<sub>2</sub>O = 6/1/5.33, methanol WHSV = 20.0 h<sup>-1</sup>, GHSV = 86 385 h<sup>-1</sup>. Reaction conditions for CT = 3.55 s: 425 °C, 4.0 MPa, H<sub>2</sub>/MEOH/H<sub>2</sub>O = 5/1/5.33, methanol WHSV = 4.0 h<sup>-1</sup>, GHSV = 15 871 h<sup>-1</sup>.

content on the deactivated catalyst is 240 mg/g. However, under the H<sub>2</sub>-absent conditions the coke formation presents a continuous and fast increase until complete deactivation (TOS = 2.5 h), giving a coke content of 185 mg/g. It is noted that the coke content is almost the same at TOS = 1.0 h under both H<sub>2</sub> and H<sub>2</sub>-absent atmospheres, implying that the inhibition effect on the coke deposition is weak at the initial reaction stage.

The evolution of coke species and quantitative results are listed in Figure S11 and Figure 6. The coke species of the H-DMTO process at 425 °C (Figure S11a) are similar to those of the normal-pressure MTO reaction at  $T \geq 400$  °C.<sup>13,25,26</sup> Figure 6b shows the variation of the coke species with different benzene rings along with the TOS under H<sub>2</sub> atmosphere. All species increase quickly during the first several hours. Afterward, the content of pyrene (four benzene rings) rises slowly with the decrease of methyl-naphthalenes (two benzene rings), whereas the content of methylbenzenes (one benzene ring) and phenanthrenes (three benzene rings) only shows small fluctuation. Under the H<sub>2</sub>-absent conditions (Figure 6c), the amount of phenanthrenes and pyrenes rises monotonously at the expense of methylbenzenes and methyl-naphthalenes. These results imply that the presence of H<sub>2</sub> in the reaction system has less suppressive effect on the formation of active intermediates (methylbenzenes and methyl-naphthalenes), which is consistent with the high content of light aromatics in the H<sub>2</sub>-treated catalyst (Figure 4). However, H<sub>2</sub> can remarkably slow down the conversion of active intermediates to heavy polycyclic aromatics.

**3.5. A Proposed Evolution Network of Coke Species in the H-DMTO Process.** A proposed evolution network of coke species is illustrated in Scheme 1. This network is built based on two considerations: carbenium ions (HCP species) are important intermediates for the formation of both olefins and polycyclic aromatics; H<sub>2</sub> could react with carbenium ions in acid solution forming electroneutral species as previously reported.<sup>6</sup> So the existence of H<sub>2</sub> in the H-DMTO process may reduce the amount of the carbenium ions because the formed carbenium ions are prone to be saturated by H<sub>2</sub> to produce hydrogenated products. With the increase of H<sub>2</sub> partial pressure, more saturated products formed, and some of them may isomerize to adamantanes and diadamantanes. Moreover, with the increase of temperature, the partial hydrogenated products and saturated ones tend to crack to smaller aromatics. This means that the hydrogenation and cracking of polycyclic

aromatic carbenium ions can be modulated by tuning H<sub>2</sub> partial pressure and reaction temperature. When a dynamic balance is built between the formation and degradation, the catalyst lifetime will be very long. As deduced from Figure 4 and Figure 6b, such a delicate balance is achieved at phenanthrene (its content was nearly unchanged after 4 h), which slows down the transformation from naphthalene to pyrene.

**3.6. H-DMTO Performance under Optimized Reaction Conditions.** By optimizing the reaction conditions such as reducing the contact time and enhancing H<sub>2</sub> and H<sub>2</sub>O partial pressures, the H-DMTO reaction performance may be further improved. Figure 7 gives the results of H-DMTO reaction with shorter contact time. The CH<sub>3</sub>OH handling capacity (MHC) of SAPO-34 shows a great increase as the CT drops from 3.55 to 0.65 s. The MHC at CT = 0.65 s is calculated to be about 203 times (based on the data of methanol conversion >96%) larger than that of the normal-pressure MTO reaction in Figure S4a. Also, lower CT facilitates improvement of the selectivity of (C<sub>2</sub>H<sub>4</sub> + C<sub>3</sub>H<sub>6</sub>) and (C<sub>2</sub>H<sub>4</sub> + C<sub>3</sub>H<sub>6</sub> + C<sub>4</sub>) as shown in Figure 7b. Moreover, we found that under conditions of lower MEOH feeding and lower total pressure, the H-DMTO reaction can proceed steadily for a long time at 400 °C (Figure S12), which is different from that at the same temperature shown in Figure 5. Possibly, low MEOH partial pressure (corresponding to low product partial pressures) is unfavorable for the formation of diadamantanes. This result implies that the formation of diadamantane species is not exclusively determined by reaction temperature; other factors such as MEOH partial pressure and MEOH WHSV may also have influence on their formation. Furthermore, the catalyst stability after the high-pressure reaction is examined by XRD analysis. It is found that the SAPO-34 framework became partially damaged after the reaction under both pure H<sub>2</sub> and H<sub>2</sub>-H<sub>2</sub>O atmospheres (Figure S13), likely caused by the steam under the reaction conditions. Further studies are needed to better understand the catalyst structure deterioration.

## 4. CONCLUSIONS

In summary, the methanol to olefins reactions under high-pressure H<sub>2</sub> and H<sub>2</sub>O atmospheres were studied systematically. Our results show that the acid sites on zeolites can catalyze the hydrogenation of aromatics under high-pressure H<sub>2</sub> atmos-

phere, which slows down the coke deposition in the MTO reaction and prolongs the catalyst lifetime. The presence of H<sub>2</sub> in the reaction system has less suppressive effect on the formation of active intermediates (methylbenzenes and methylnaphthalenes) but can remarkably retard the conversion of active intermediates to heavy polycyclic aromatics with a delicate balance at phenanthrene. Water is beneficial for the lifetime improvement, and higher H<sub>2</sub>O partial pressure can help enhance the hydrogenation ability of SAPO-34 in the H-DMTO process. The H-DMTO reaction lifetime is also sensitive to the reaction temperature. The evolution pathways of coke species may change at temperature of lower than 400 °C, leading to the formation of large molecule diadamantanes and thus a fast catalyst deactivation. The present findings shed light on the hydrogenation function of acidic zeolites and give a plausible explanation on the long lifetime of SAPO-34 in STO reaction. More importantly, it provides a new way to improve the catalyst lifetime for zeolite-catalyzed hydrocarbon conversions.

## ■ ASSOCIATED CONTENT

### Supporting Information

The Supporting Information is available free of charge on the ACS Publications website at DOI: [10.1021/acscatal.8b04402](https://doi.org/10.1021/acscatal.8b04402).

Catalyst characterization and additional results (PDF)

## ■ AUTHOR INFORMATION

### Corresponding Authors

\*E-mail: [liuzm@dicp.ac.cn](mailto:liuzm@dicp.ac.cn) (Z.L.).

\*E-mail: [tianpeng@dicp.ac.cn](mailto:tianpeng@dicp.ac.cn) (P.T.).

### ORCID

Xinwen Guo: 0000-0002-6597-4979

Zhongmin Liu: 0000-0001-8439-2336

### Author Contributions

<sup>1</sup>X.Z. and J.L. contributed equally to this work.

### Notes

The authors declare no competing financial interest.

## ■ ACKNOWLEDGMENTS

The authors are thankful for the financial support from the National Natural Science Foundation of China (No. 21676262 and No. 21576256) and the Key Research Program of Frontier Sciences, CAS (QYZDB-SSW-JSC040). Dedicated to the 70th anniversary of Dalian Institute of Chemical Physics, CAS.

## ■ REFERENCES

- (1) Blay, V.; Louis, B.; Miravalles, R.; Yokoi, T.; Peccatiello, K. A.; Clough, M.; Yilmaz, B. Engineering Zeolites for Catalytic Cracking to Light Olefins. *ACS Catal.* **2017**, *7*, 6542–6566.
- (2) Kanai, J.; Martens, J. A.; Jacobs, P. A. On the nature of the active-sites for ethylene hydrogenation in metal-free zeolites. *J. Catal.* **1992**, *133*, 527–543.
- (3) Vityuk, A.; Aleksandrov, H. A.; Vayssilov, G. N.; Alexeev, O. S.; Amiridis, M. D.; Khivantsev, K. Room Temperature Ethene Hydrogenation Activity of Transition-Metal-Free HY Zeolites. *ACS Catal.* **2019**, *9*, 839–847.
- (4) Senger, S.; Radom, L. Zeolites as transition-metal-free hydrogenation catalysts: A theoretical mechanistic study. *J. Am. Chem. Soc.* **2000**, *122*, 2613–2620.
- (5) Siria, J. C.; Duran, M.; Lledos, A.; Bertran, J. Acid-catalyzed hydrogenation of olefins - a theoretical study of the HF-catalyzed and H<sub>3</sub>O<sup>+</sup>-catalyzed hydrogenation of ethylene. *J. Am. Chem. Soc.* **1987**, *109*, 7623–7629.
- (6) Wristers, J. Strong acid-catalyzed hydrogenation of aromatics. *J. Am. Chem. Soc.* **1975**, *97*, 4312–4316.
- (7) Tian, P.; Wei, Y.; Ye, M.; Liu, Z. Methanol to Olefins (MTO): From Fundamentals to Commercialization. *ACS Catal.* **2015**, *5*, 1922–1938.
- (8) Dahl, I. M.; Kolboe, S. On the reaction mechanism for hydrocarbon formation from methanol over SAPO-34: I. isotopic labeling studies of the co-reaction of ethene and methanol. *J. Catal.* **1994**, *149*, 458–464.
- (9) Dahl, I. M.; Kolboe, S. On the reaction mechanism for hydrocarbon formation from methanol over SAPO-34 0.2. Isotopic labeling studies of the co-reaction of propene and methanol. *J. Catal.* **1996**, *161*, 304–309.
- (10) Xu, S.; Zhi, Y.; Han, J.; Zhang, W.; Wu, X.; Sun, T.; Wei, Y.; Liu, Z. Advances in Catalysis for Methanol-to-Olefins Conversion. *Adv. Catal.* **2017**, *61*, 37–122.
- (11) Mikkelsen, O.; Ronning, P. O.; Kolboe, S. Use of isotopic labeling for mechanistic studies of the methanol-to-hydrocarbons reaction. Methylation of toluene with methanol over H-ZSM-5, H-mordenite and H-beta. *Microporous Mesoporous Mater.* **2000**, *40*, 95–113.
- (12) Haw, J. F.; Nicholas, J. B.; Song, W. G.; Deng, F.; Wang, Z. K.; Xu, T.; Heneghan, C. S. Roles for cyclopentenyl cations in the synthesis of hydrocarbons from methanol on zeolite catalyst HZSM-5. *J. Am. Chem. Soc.* **2000**, *122*, 4763–4775.
- (13) Haw, J. F.; Song, W. G.; Marcus, D. M.; Nicholas, J. B. The mechanism of methanol to hydrocarbon catalysis. *Acc. Chem. Res.* **2003**, *36*, 317–326.
- (14) Jiao, F.; Li, J.; Pan, X.; Xiao, J.; Li, H.; Ma, H.; Wei, M.; Pan, Y.; Zhou, Z.; Li, M.; Miao, S.; Li, J.; Zhu, Y.; Xiao, D.; He, T.; Yang, J.; Qi, F.; Fu, Q.; Bao, X. Selective conversion of syngas to light olefins. *Science* **2016**, *351*, 1065–1068.
- (15) Cheng, K.; Gu, B.; Liu, X.; Kang, J.; Zhang, Q.; Wang, Y. Direct and highly selective conversion of synthesis gas into lower olefins: design of a bifunctional catalyst combining methanol synthesis and carbon-carbon coupling. *Angew. Chem., Int. Ed.* **2016**, *55*, 4725–4728.
- (16) Jiao, F.; Pan, X.; Gong, K.; Chen, Y.; Li, G.; Bao, X. Shape-Selective Zeolites Promote Ethylene Formation from Syngas via a Ketene Intermediate. *Angew. Chem., Int. Ed.* **2018**, *57*, 4692–4696.
- (17) Liu, X.; Zhou, W.; Yang, Y.; Cheng, K.; Kang, J.; Zhang, L.; Zhang, G.; Min, X.; Zhang, Q.; Wang, Y. Design of efficient bifunctional catalysts for direct conversion of syngas into lower olefins via methanol/dimethyl ether intermediates. *Chem. Sci.* **2018**, *9*, 4708–4718.
- (18) Nieskens, D. L. S.; Lunn, J. D.; Malek, A. Understanding the Enhanced Lifetime of SAPO-34 in a Direct Syngas-to-Hydrocarbons Process. *ACS Catal.* **2019**, *9*, 691–700.
- (19) Ni, Y.; Chen, Z.; Yang, M.; Liu, H.; He, Y.; Fu, Y.; Zhu, W.; Liu, Z.; Liu, Y. Realizing and Recognizing Syngas-to-olefins Reaction via a Dual-bed Catalyst. *ACS Catal.* **2019**, *9*, 1026.
- (20) Chowdhury, A. D.; Paioni, A. L.; Houben, K.; Whiting, G. T.; Baldus, M.; Weckhuysen, B. M. Bridging the gap between the direct and hydrocarbon pool mechanisms of the methanol-to-hydrocarbons process. *Angew. Chem., Int. Ed.* **2018**, *57*, 8095–8099.
- (21) Arora, S. S.; Nieskens, D. L. S.; Malek, A.; Bhan, A. Lifetime improvement in methanol-to-olefins catalysis over chabazite materials by highpressure H<sub>2</sub> co-feeds. *Nat. Catal.* **2018**, *1*, 666–672.
- (22) Yarulina, I.; De Wispelaere, K.; Bailleul, S.; Goetze, J.; Radersma, M.; Abou-Hamad, E.; Vollmer, I.; Goesten, M.; Mezari, B.; Hensen, E. J. M.; Martinez-Espin, J. S.; Morten, M.; Mitchell, S.; Perez-Ramirez, J.; Olsbye, U.; Weckhuysen, B. M.; Van Speybroeck, V.; Kapteijn, F.; Gascon, J. Structure-performance descriptors and the role of Lewis acidity in the methanol-to-propylene process. *Nat. Chem.* **2018**, *10*, 804–812.
- (23) Yarulina, I.; Chowdhury, A. D.; Meirer, F.; Weckhuysen, B. M.; Gascon, J. Recent trends and fundamental insights in the methanol-to-hydrocarbons process. *Nat. Catal.* **2018**, *1*, 398–411.
- (24) De Wispelaere, K.; Wondergem, C. S.; Ensing, B.; Hemelsoet, K.; Meijer, E. J.; Weckhuysen, B. M.; Van Speybroeck, V.; Ruiz-



Martinez, J. Insight into the Effect of Water on the Methanol-to-Olefins Conversion in H-SAPO-34 from Molecular Simulations and in Situ Microspectroscopy. *ACS Catal.* **2016**, *6*, 1991–2002.

(25) Bleken, F.; Bjorgen, M.; Palumbo, L.; Bordiga, S.; Svelle, S.; Lillerud, K.-P.; Olsbye, U. The Effect of Acid Strength on the Conversion of Methanol to Olefins Over Acidic Microporous Catalysts with the CHA Topology. *Top. Catal.* **2009**, *52*, 218–228.

(26) Chen, J.; Li, J.; Wei, Y.; Yuan, C.; Li, B.; Xu, S.; Zhou, Y.; Wang, J.; Zhang, M.; Liu, Z. Spatial confinement effects of cage-type SAPO molecular sieves on product distribution and coke formation in methanol-to-olefin reaction. *Catal. Commun.* **2014**, *46*, 36–40.

(27) Arora, S. S.; Bhan, A. The critical role of methanol pressure in controlling its transfer dehydrogenation and the corresponding effect on propylene-to-ethylene ratio during methanol-to-hydrocarbons catalysis on H-ZSM-5. *J. Catal.* **2017**, *356*, 300–306.

(28) Hwang, A.; Kumar, M.; Rimer, J. D.; Bhan, A. Implications of methanol disproportionation on catalyst lifetime for methanol-to-olefins conversion by HSSZ-13. *J. Catal.* **2017**, *346*, 154–160.

(29) Hill, I. M.; Al Hashimi, S.; Bhan, A. Kinetics and mechanism of olefin methylation reactions on zeolites. *J. Catal.* **2012**, *285*, 115–123.

(30) Mueller, S.; Liu, Y.; Vishnuvarthan, M.; Sun, X.; van Veen, A. C.; Haller, G. L.; Sanchez-Sanchez, M.; Lercher, J. A. Coke formation and deactivation pathways on H-ZSM-5 in the conversion of methanol to olefins. *J. Catal.* **2015**, *325*, 48–59.

(31) Marchi, A. J.; Froment, G. F. Catalytic conversion of methanol to light alkene on SAPO molecular-sieves. *Appl. Catal.* **1991**, *71*, 139–152.

(32) Wu, X. C.; Anthony, R. G. Effect of feed composition on methanol conversion to light olefins over SAPO-34. *Appl. Catal., A* **2001**, *218*, 241–250.

(33) Smith, L.; Cheetham, A. K.; Morris, R. E.; Marchese, L.; Thomas, J. M.; Wright, P. A.; Chen, J. On the nature of water bound to a solid acid catalyst. *Science* **1996**, *271*, 799–802.

(34) Stanislaus, A.; Cooper, B. H. Aromatic hydrogenation catalysis: A review. *Catal. Rev.: Sci. Eng.* **1996**, *38*, 159–159.

(35) Siskin, M. Strong acid chemistry. 2. catalytic -hydrogenation of aromatics in hydrogen fluoride-tantalum pentafluoride and related strong acid systems. *J. Am. Chem. Soc.* **1974**, *96*, 3641–3641.

(36) Segawa, Y.; Stephan, D. W. Metal-free hydrogenation catalysis of polycyclic aromatic hydrocarbons. *Chem. Commun.* **2012**, *48*, 11963–11965.

(37) Garnica, M. M.; Torres, A. E.; Ramirez-Caballero, G. E.; Balbuena, P. B. Exploring the acid catalyzed isomerization of phenanthrene under confinement in mordenite. *Microporous Mesoporous Mater.* **2018**, *265*, 241–249.

(38) Wei, Y.; Yuan, C.; Li, J.; Xu, S.; Zhou, Y.; Chen, J.; Wang, Q.; Xu, L.; Qi, Y.; Zhang, Q.; Liu, Z. Coke Formation and Carbon Atom Economy of Methanol-to-Olefins Reaction. *ChemSusChem* **2012**, *5*, 906–912.